ELSEVIER

Journal of Structural Geology 30 (2008) 291–309

JOURNAL OF STRUCTURAL GEOLOGY

www.elsevier.com/locate/jsg

Foliation boudinage

Arzu Arslan*, Cees W. Passchier, Daniel Koehn

Tectonophysics, Institute of Geosciences, University of Mainz, Becherweg 21, 55099 Mainz, Germany

Received 27 June 2007; received in revised form 5 November 2007; accepted 12 November 2007
Available online 19 November 2007

Abstract

Foliation boudinage is a form of boudinage that develops in foliated rocks independent of lithology contrast. This paper describes foliation boudins from the Çine Massif in SW Turkey and the Furka Pass–Urseren Zone in central Switzerland. Four common types of foliation boudin structures can be distinguished in the field, named after vein geometries in their boudin necks in sections normal to the boudin axis: lozenge-, crescent-, X- and double crescent-type. The boudin necks are mostly filled with massive quartz in large single crystals, commonly associated with tourmaline, feldspar and biotite and in some cases with chlorite spherulites. The presence of blocky crystals and chlorite spherulites suggests that these veins formed as open, fluid-filled cavities during the initiation and development of foliation boudin structures, even in ductilely deforming gneiss at a depth of mid-crustal levels (7–10 kbar). The presence of cavities allowed the formation of closed fishmouth structures that are typical for many foliation boudins. The geometry of foliation boudin structures mainly depends on initial fracture orientation, propagation of the fracture during further deformation, and flow type in the wall rock.

Keywords: Foliation boudinage; Vein; Shear zone; Çine Massif; Urseren Zone

1. Introduction

Boudinage is a common phenomenon in layered rocks, where layers of a specific lithology are disrupted into elongate fragments. Such separation can develop by planar fracturing into rectangular fragments (torn boudins) or by necking and tapering into elongate depressions and swells known as drawn boudins (Goscombe et al., 2004: Fig. 1). Where the boudins are separated by fractures or vein material, the separation zones are known as boudin necks. In some types of torn boudins, and in all drawn boudins, the layers are deflected into the boudin neck in a characteristic geometry (Goscombe et al., 2004: Fig. 1). In some cases, the deflection can be so strong that the upper and lower contact of a layer touches in the boudin neck. If this occurs by infolding of the original fracture, the developing structure is known as a ''fishmouth boudin'' where the deformed fracture forms the ''mouth'' of the ''fish'' (Goscombe et al., 2004: Fig. 1). Boudin necks normally occur in a series of similar structures along a layer with regular spacing, separating the layer into ''boudins''. This type of layer-restricted boudinage is thought to result from differences in rheology between a relatively stiff layer and a viscous matrix, where the stiff layer ruptures or necks normal to the extension direction in the rock (e.g. Ramberg, 1955; Strömgård, 1973; Lloyd and Ferguson, 1981; Lloyd et al., 1982; Ramsay and Huber, 1983).

Besides this usual type of boudinage, similar structures are observed in foliated rocks that do not have layering. Many strongly foliated rocks show veins at a high angle to the foliation plane with a deflection of the foliation into the veins similar to that of boudin necks in layering (Fig. 1). Because of this similarity and the apparent link to foliated rocks, this type of structure is known as ''foliation boudinage'' (Hambrey and Milnes, 1975; Platt and Vissers, 1980). There is a continuum in ''layeredness'' between foliation boudinage through multi-layer-boudinage of successively thicker planes to true layer-boudinage (Goscombe et al., 2004).

In layer-boudinage, boudin blocks can be easily defined as distinct elongate fragments of the competent layer. Foliation

* Corresponding author. Tel.: +49 6131 39 24767; fax: +49 6131 39 23863.
E-mail address: arslan@uni-mainz.de (A. Arslan).

0191-8141/$ - see front matter © 2007 Elsevier Ltd. All rights reserved.
doi:10.1016/j.jsg.2007.11.004

Fig. 1. Foliation boudinage structure (FBS) in augen gneiss, the Çine Massif, SW Turkey. The geometry of the boudin neck is a typical fishmouth. Vein fill is massive quartz. Location: Asmaköy (37°43′33N; 28°26′42E).

boudinage occurs at isolated sites in foliated rocks, and is not generally related to any apparent rheologically contrasting layer (Fig. 1). As a result, the prominent elements of foliation boudinage are not the boudins, but the neck regions. In this paper we will therefore mostly avoid the term ''foliation boudin'' and either use the term ''foliation boudinage'' for the process or ''foliation boudinage structure (FBS)'' for the structure in the necks.

Foliation boudinage was first analysed by Cobbold et al. (1971), who studied the behaviour of homogeneous, anisotropic rocks during layer normal compression and suggested that internal instabilities lead to the development of boudin-like structures. They referred to these as ''internal boudinage''. The term ''foliation boudinage'' was first used by Hambrey and Milnes (1975) to describe boudin-like structures in glacier ice, which shows a strong planar anisotropy or foliation. Platt and Vissers (1980) described the phenomenon in homogeneous rock masses that are strongly anisotropic. Aerden (1991) stressed the economic importance of foliation boudinage since it commonly controls ore bodies. A number of studies have shown that FBSs can also be used as shear sense indicators (e.g. Platt and Vissers, 1980; Hanmer, 1986; Lacassin, 1988; Swanson, 1992; Grasemann and Stüwe, 2001; Goscombe and Passchier, 2003; Grasemann et al., 2003). Analogue modelling by Druguet and Carreras (2006) presents the important role of rheological change through melt crystallization during deformation.

In this paper, we describe and classify different types of foliation boudinage structures from the Çine Massif, SW Turkey and the Furka Pass–Urseren Zone, Central Switzerland, where FBSs are particularly common. We have chosen to investigate structures from two areas with different tectonic regime, protolith and metamorphic grade in order to see if our observations have general validity. Our aim is to investigate if and how the geometry of FBS is dependent on foliation strength, rock type, flow regime and other parameters. Formation mechanisms of FBSs are discussed based on field observations and on numerical modelling.

2. Study areas

2.1. Geology of the Çine submassif

The Çine submassif is part of the Menderes Metamorphic Core Complex (MMCC) in western Turkey (Fig. 2). The MMCC consists of a core of tectonic units known as the Menderes nappes (Ring et al., 1999) of mainly orthogneiss and micaschist of Neoproterozoic to Palaeozoic age tectonically overlain by a number of other thrust sheets. The highest units are the Ízmir–Ankara Zone of Neotethys in the north (Sengör and Yılmaz, 1981) and the Lycian nappes of the Taurides in the south (Graciansky, 1968; Bernoulli et al., 1974), which consist of dominantly Permo-Mesozoic passive margin successions and ophiolitic mélange. The underlying Dilek nappe and Selçuk melange (Güngör, 1998 and the references therein) have been correlated to the Cycladic blueschist unit (Candan et al., 1997; Ring et al., 1999; Gessner, 2000) and consist of a Mesozoic platform sequence with emery- and rudist-bearing marbles and overlying metaolistostromes. The Menderes nappes are, from highest to lowest structural level, the Selimiye, Çine, Bozdag and Bayındır nappes (Fig. 2a). The nappes were emplaced during the Late Cretaceous to Tertiary and later underwent Tertiary to recent regional extensional deformation. This extension by vertical shortening and N–S horizontal extension in the nappes, caused development of foliations, lineations, boudins and related structures, and later formed the E–W trending grabens which dissect the region into three submassifs: from north to south the Gördes, Ödemis and Çine submassifs. This study focuses on the Çine submassif, and specifically on the structures in mylonitised granitoid and metasedimentary rocks of the Çine nappe (Fig. 2).

Gessner et al. (2001) divided granitic rocks of the Çine nappe into older orthogneiss and younger meta-granites that have yielded Neoproterozoic to Cambrian ages (Kröner and Sengör, 1990; Hetzel and Reischmann, 1996; Loos and Reischmann, 1999; Gessner et al., 2004). However, a Tertiary age has also been suggested for gneissic granites along the southern margin of the Çine submassif due to an intrusive contact with Mesozoic micaschist (Bozkurt, 2004; Erdogan and Güngör, 2004).

Although the contact relations between the units, the age of metamorphism and deformation are still subject to discussion, there is general consensus on an early top-to-N/NE shear sense in orthogneiss and metasedimentary rocks of the Çine nappe during amphibolite facies metamorphism, overprinted by top-to-South shear sense during greenschist facies metamorphism (Gessner et al., 2001; Régnier et al., 2003, 2007; Bozkurt and Satır, 2000; Bozkurt, 2007; Bozkurt et al., 2006). Régnier et al. (2003) recorded maximum P–T conditions of about 7 kbar and >550 °C for the metasedimentary rocks of the Çine nappe underneath the Selimiye shear zone and 8–11 kbar and 600–650 °C in the north for the same

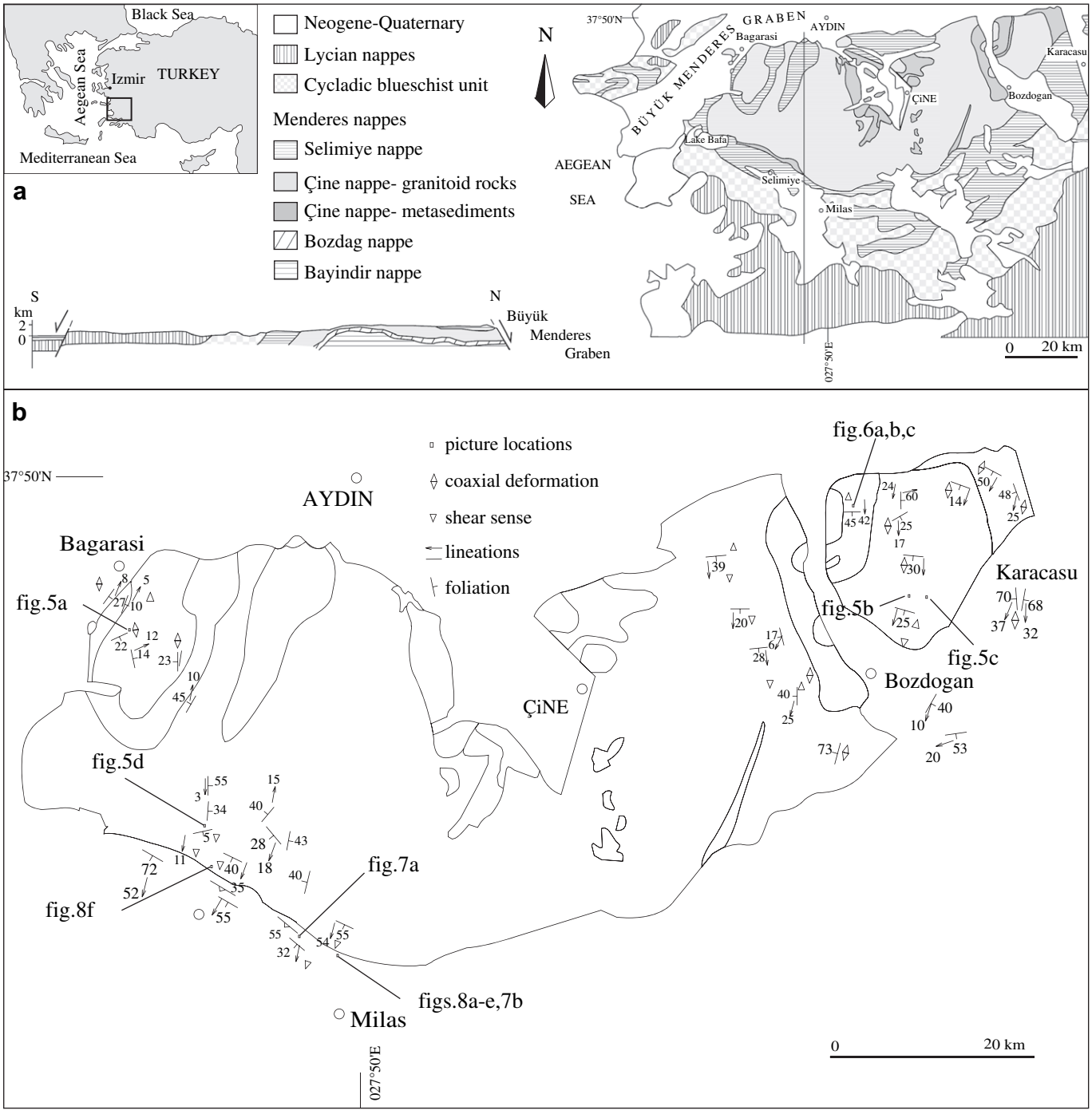

Fig. 2. Location of the study area in SW Turkey. (a) Simplified geological map and cross-section after Candan and Dora (1997) and Gessner et al. (2001). (b) Measurements of foliation and lineation in gneiss where foliation boudinage structures have been investigated. Locations of figures in the text are shown.

rocks. Similar P–T conditions of 8–10 kbar and 600–640 °C were also reported for the metasedimentary enclaves in the orthogneiss in the western Çine Massif by Régnier et al. (2007). The metamorphic conditions in the orthogneiss were defined by the fabrics which seem to have formed above 500 °C (Gessner et al., 2001). Variable shear sense in the orthogneiss, with top-to-the-North in the north and top-to-the-South in the south and with local coaxial deformation, was attributed to strain partitioning by Régnier et al. (2007).

Foliation boudinage structures are common in both orthogneiss and micaschist of the Çine nappe. The orthogneiss is granodioritic in composition and contains cm-scale feldspar augen surrounded by a biotite foliation. The foliation is subhorizontal in the central part of the Çine submassif and aggregate lineations are well developed and generally N–S trending but gradually become steeper to the south, especially along the southern margin in the Selimiye shear zone (Fig. 2b). The micaschist is a biotite–garnet micaschist with

indications of retrogression in the form of chlorite veins. Alteration of garnet and biotite to chlorite is common.

2.2. Geology of the Furka Pass–Urseren Zone

The Furka Pass–Urseren Zone between the Aar- and Gotthard massifs is a narrow zone in the Infra-Helvetic Complex, north of the Lepontine Metamorphic Dome and the Periadriatic Line and north–northeast of the Simplon Fault Zone, in Central Switzerland (Fig. 3). The massifs, mainly late Variscan granites and old crystalline rocks together with narrow zones of Carboniferous sediments and volcanics, form the pre-Mesozoic basement of the Helvetic nappes and are the northernmost exposures of the external crystalline massifs. They represent updomed basement nappes separated by their Mesozoic sedimentary cover and by the basal Glarus thrust from the overlying Helvetic nappes (Milnes and Pfiffner, 1977). The basement has partially been reworked by the Variscan and Alpine orogenesis. The pre-Alpine evolution, including Variscan, Ordovician and Precambrian events, has been reported in detail by many workers (e.g. Albrecht et al., 1991; Albrecht, 1994; Schaltegger, 1994; Schaltegger and Gebauer, 1999; von Raumer et al., 1999; and references therein). In the southern Aar Massif, Alpine overprint was strong and the basement and cover rocks were affected by ductile deformation under greenschist facies metamorphism with P/T conditions of 300–450 °C and 3–4.5 kbar increasing from north to south and further south in the Gotthard Massif reaching amphibolite facies (Marquer and Burkhard, 1992; Frey and Mahlmann, 1999). The geometry of this heterogeneous deformation shows anastomosing patterns of shear zones corresponding to a bulk vertical stretching. For the southern Aar Massif 450 °C and 4.4 kbar conditions are constrained by fluid inclusion data from fissure quartz (Frey and Mahlmann, 1999).

We studied foliation boudinage structures in the mylonitic gneisses and metasediments of the Furka Pass–Urseren Zone that have an approximately NE–SW striking and vertical to steeply dipping regional penetrative foliation (Fig. 3a,b). The aggregate and grain lineations are mostly vertical or steeply plunging. Both structures formed in anastomosing shear zones with a vertical displacement component. However in some narrow shear zones evidence for a strike-slip component of motion is found.

3. Foliation boudinage structures (FBSs)

3.1. Foliation boudinage structures (FBSs) in the Çine submassif

Foliation boudinage structures (FBSs) are isolated structures in rocks recognized by perturbations in the monotonous foliation adjacent to a central discontinuity, mostly filled with

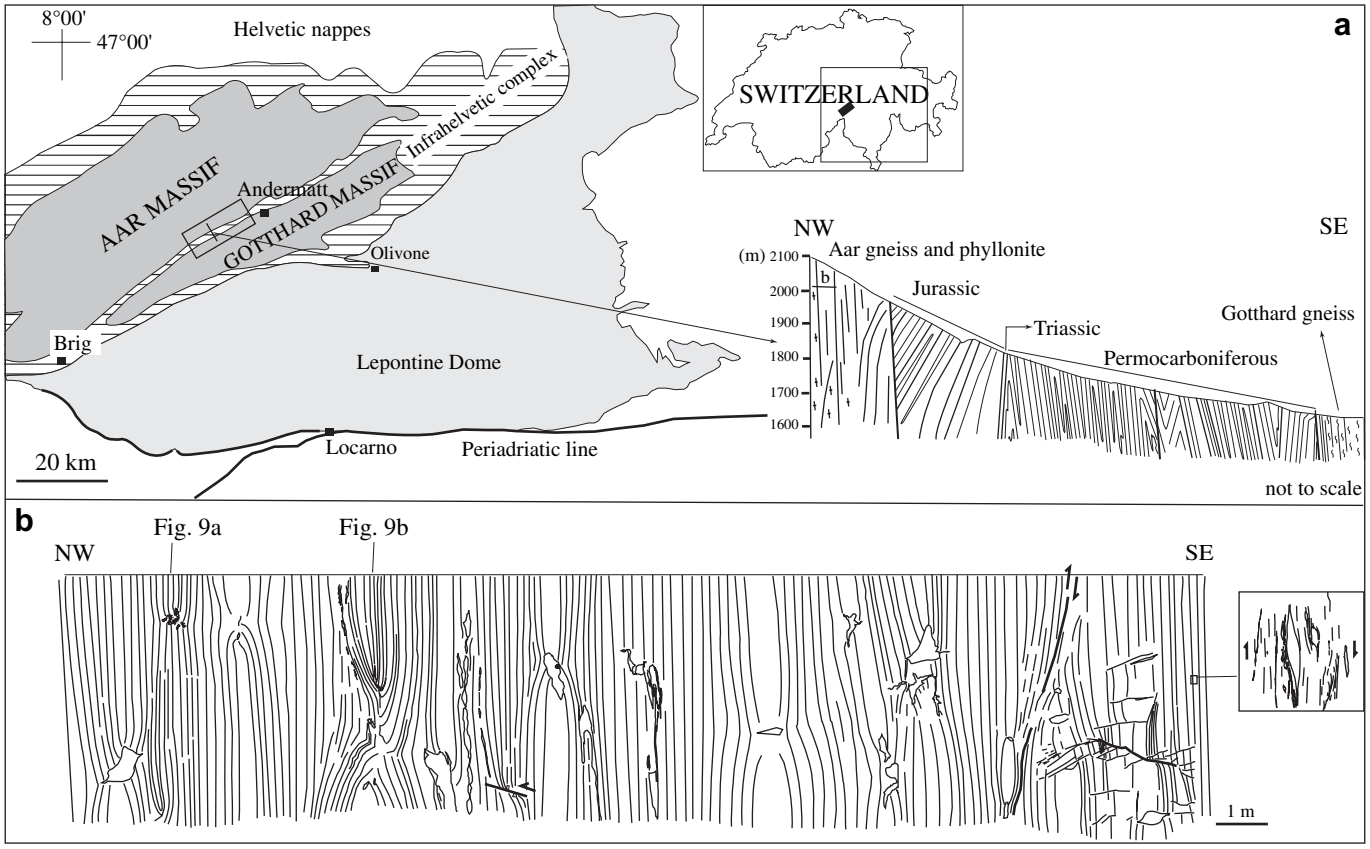

Fig. 3. (a) Location of the area in Switzerland where foliation boudinage structures were studied. Simplified geological map and cross-section modified after Lebit (1989). (b) Sketches of FBSs along a short road-cut section opposite the Belvedere Hotel, Furka Pass.

vein material. The planar foliation and straight lineation in the far-field wall rock are deflected close to the central discontinuity, and the typical shape of a foliation boudinage structure as described below is defined by the deflection pattern of the foliation, and the shape of the central veins. The deflection pattern close to a central vein is a category of flanking folds (Passchier, 2001). Boudin neck veins are normally structures with an elongate, commonly curved disc-shaped geometry; the longest axis (L_b) is parallel to the foliation and typically normal to the aggregate lineation (L) in the rock and the shorter axis normal or oblique to the foliation (Fig. 4).

We have applied and in some cases adapted the boudin terminology of Goscombe and Passchier (2003) to describe the geometry of FBSs (Fig. 4). Since most of the FBSs in the studied area have mineral-filled boudin neck veins, an interboudin surface (S_{ib}; Goscombe and Passchier, 2003) is defined as an imaginary median surface passing through the centre of the neck vein. Symmetry of FBSs can be easily recognized when these interboudin surfaces (S_{ib}) are drawn. The angle θ between S_{ib} and the main foliation is between 50° and 90° changing with different FBS types.

Since there is no boudinaged single competent layer, a boudin exterior S_b is defined here as a foliation plane that starts at the vein tips, extends away from the vein and becomes parallel to the external, far-field foliation (f_e); f_e is the main penetrative foliation in the host rock and is not affected by perturbations around the vein. The foliation affected by perturbations adjacent to the vein, described in Passchier (2001) as internal

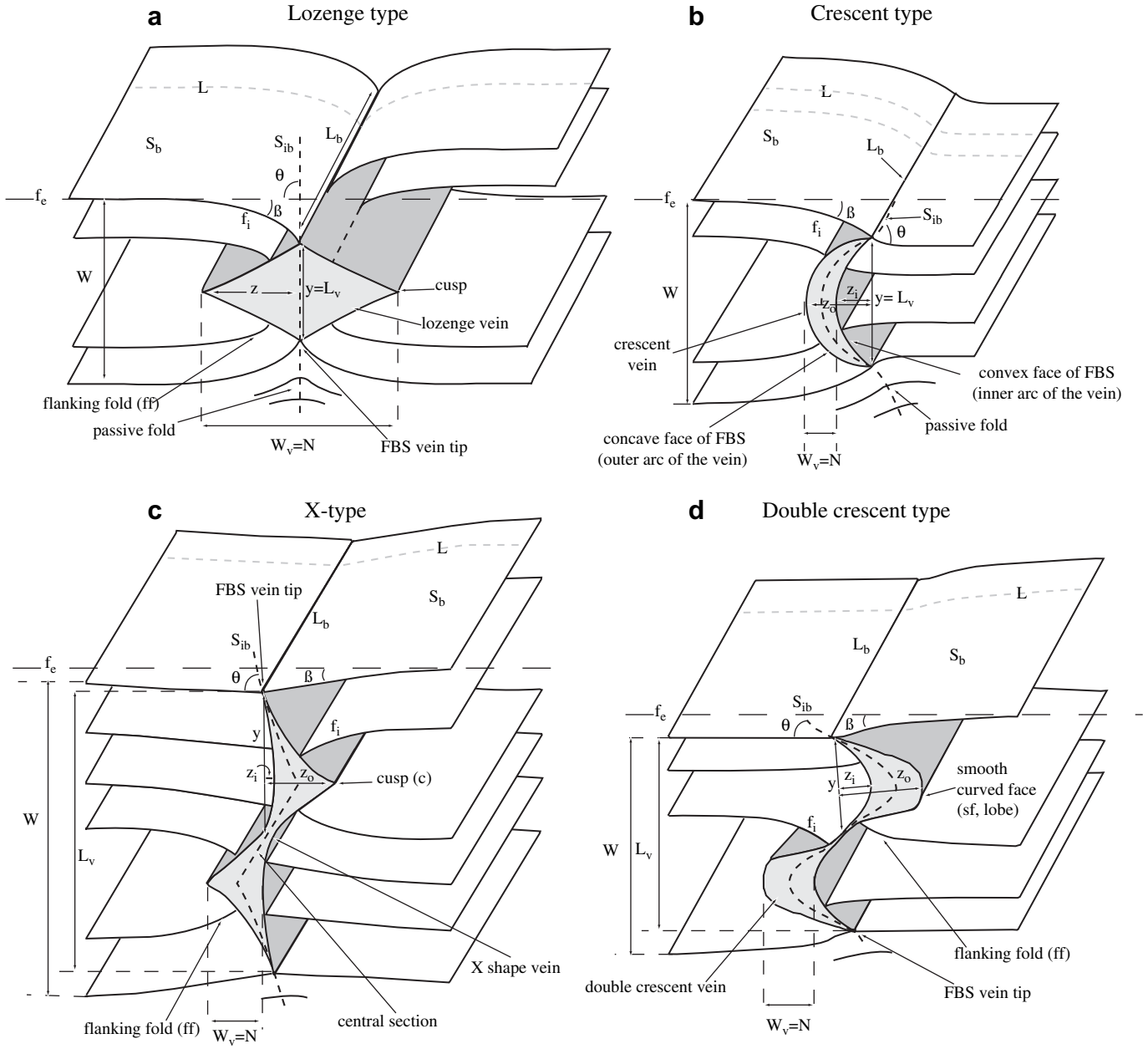

Fig. 4. Geometry of foliation boudinage structures (FBSs). (a) Lozenge-type. (b) Crescent-type. (c) X-type. (d) Double crescent-type. See text for explanation.

host element (HE_i), is here referred to as the internal foliation (f_i). The deflection of the foliation, measured as an angle β, is the deviation of the internal foliation from its external, f_e orientation (Figs. 4 and 5e). There is a gradual transition between f_i and f_e.

A large number of foliation boudinage structures were analysed in the Çine Massif, ranging in size from cm- to m-scale. Both symmetric and asymmetric types of FBSs are common. Symmetrical FBSs at the northwestern margin of the Çine Massif were first mentioned by Gessner et al. (2001) and Régnier et al. (2003) as amphibolite facies structures. Boudin neck veins strike approximately E–W relative to N–S oriented aggregate lineations. The axial planes of boudin veins crosscut the regional foliation at steep angles.

On sections parallel to the aggregate lineation and normal to the foliation in the rocks, both symmetric and asymmetric types of FBSs occur and several hundred were investigated in the Çine Massif (Fig. 5). We classified the common types of foliation boudinage structures into four categories; lozenge-, crescent-, X- and double crescent-type FBSs (Figs. 4 and 5). These categories are easily distinguished in the field and are named after vein geometries in the boudin necks in cross-sections normal to the foliation and parallel to the aggregate lineation.

Lozenge- and X-type FBSs have sharp, angular vein geometries whereas crescent- and double crescent-type FBSs have smooth, curved vein geometries (Figs. 4–6). The curve of the FBSs neck vein reflects the geometry of FBS faces and these faces can be concave and convex/concave with respect to the boudin interior. The curve of the FBS faces can be defined by a ratio z/y (Goscombe et al., 2004) where z is a maximum normal deviation of the FBS face out of or into the FBS interior from a straight line connecting the edges of the FBS face at the vein tips. y is a measure of the length between the vein tips passing through the centre of the vein (Fig. 4). In the case of X- and double crescent-types, y is measured from the vein tip to the centre of the structure instead, since both are paired structures. z is measured for both inner and outer arc/curve as z_i and z_o, respectively. The inner arc can be straight if the deviation z of that face is zero, or curved. The maturity of the curvature through progressive deformation can be defined by this ratio as it decreases and approaches zero when the geometry reaches that of a closed fishmouth.

Lozenge-type FBSs are symmetric and characterized by lozenge-shaped veins in their boudin neck with two cusps facing opposite sides (Figs. 4a and 5a). A straight S_{ib} passing through the tips of the neck vein divides the structure into two symmetric parts and is at a high angle ($\theta = 90°$) to the external foliation f_e. The sharp, strongly curved vein faces also reflect the boudin face geometries known as fishmouth structures. The length/width (L_v/W_v) ratios of the boudin neck veins are low. They are known as short-type FBSs. Foliation boudin exteriors, S_b, are straight and parallel to each other on both sides except close to the neck vein.

In lozenge-type FBS, a symmetrical pair of flanking folds occurs on the two sides of the vein. The shape of these folds can be measured along single foliation planes and through the cross-section in different foliation planes. The angle β increases towards the vein cusps and decreases to the vein tips (Figs. 4a and 5a). The maximum value of β is reached near the cusp, while at the cusp it is zero in a symmetric structure. Contours for these angles can be drawn to define the exact shape of the folds (e.g. Fig. 5e). At the end of the vein tips (top and bottom) the foliation is passively folded. The degree of the curvature of these passive folds decreases away from the vein tips and becomes parallel to the straight foliation in the far field (Figs. 4a and 5e). Passive folds are common in other types of FBSs as well.

Crescent-type FBSs are asymmetric with a single smoothly curved vein in the boudin neck, with curving vein contacts facing to one side (Figs. 4b and 5b). S_{ib} is curved but close to the vein tips it is at a high angle or is normal to the foliation. FBS neck veins have high length/with ratios. Two ratios are measured to define the curve of the FBS faces for the asymmetric types: z_o/y for the outer arc of the vein and z_i/y for the inner arc. z_o is the maximum normal distance from the outer arc of the vein to the straight line connecting the vein tips while z_i is the maximum normal distance from the inner arc of the vein to this line. The length y is measured between the vein tips. Foliation bends into the outer arc of the vein and bends slightly out along the inner part.

X- and double crescent-type FBSs are asymmetric (Figs. 4c,d and 5c,d). These structures are similar to the dilational forked-gash asymmetric boudins and sigmoidal-type asymmetric boudins in layers, as described by Goscombe et al. (2004). The geometry of the neck veins resembles that of cuspate–lobate structures. FBS neck veins have high length/width ratios and are long FBS types. X-type FBSs have veins in the boudin necks with two cusps facing opposite sides similar to the lozenge-type, but here cusps are not opposite each other. S_{ib} is sharp with central and outer sections, X- or Z-shaped and in the central section at a high angle to the foliation (Figs. 4c, 5c and 6a,c). Asymmetric flanking structures are present at the ''cusped'' faces of the veins and the foliation is at a high angle to the contact on the opposite straight (Fig. 6a) or slightly curved (Figs. 5c and 6c) faces. On the side of the cusps, the deviation of the foliation (β) increases from 0° close to the vein tips to 40° near the cusps. The maximum deviation angles are found near cusps. The cusps commonly develop into fishmouth structures (Fig. 6b). On the opposite, slightly curved faces β does not deviate much from zero.

The most regular double crescent- and X-type FBSs are in fact two linked, stacked symmetric half-boudin structures with opposite polarity (Fig. 4), but we prefer to refer to the entire structure as ''asymmetric'' in our classification.

For the X- and double crescent-type the curve of the FBS faces is measured as two ratios (z_o/y and z_i/y) as for crescent types. y is a measure of length between the vein tip and the vein centre along the straight line connecting vein tips (Fig. 4c,d). Double crescent-type FBSs have double curved veins with lobes in the neck facing opposite sides (Figs. 4d and 5d). S_{ib} is smooth and sigmoidal. In the central part of the vein S_{ib} is at a higher angle to the foliation than at the

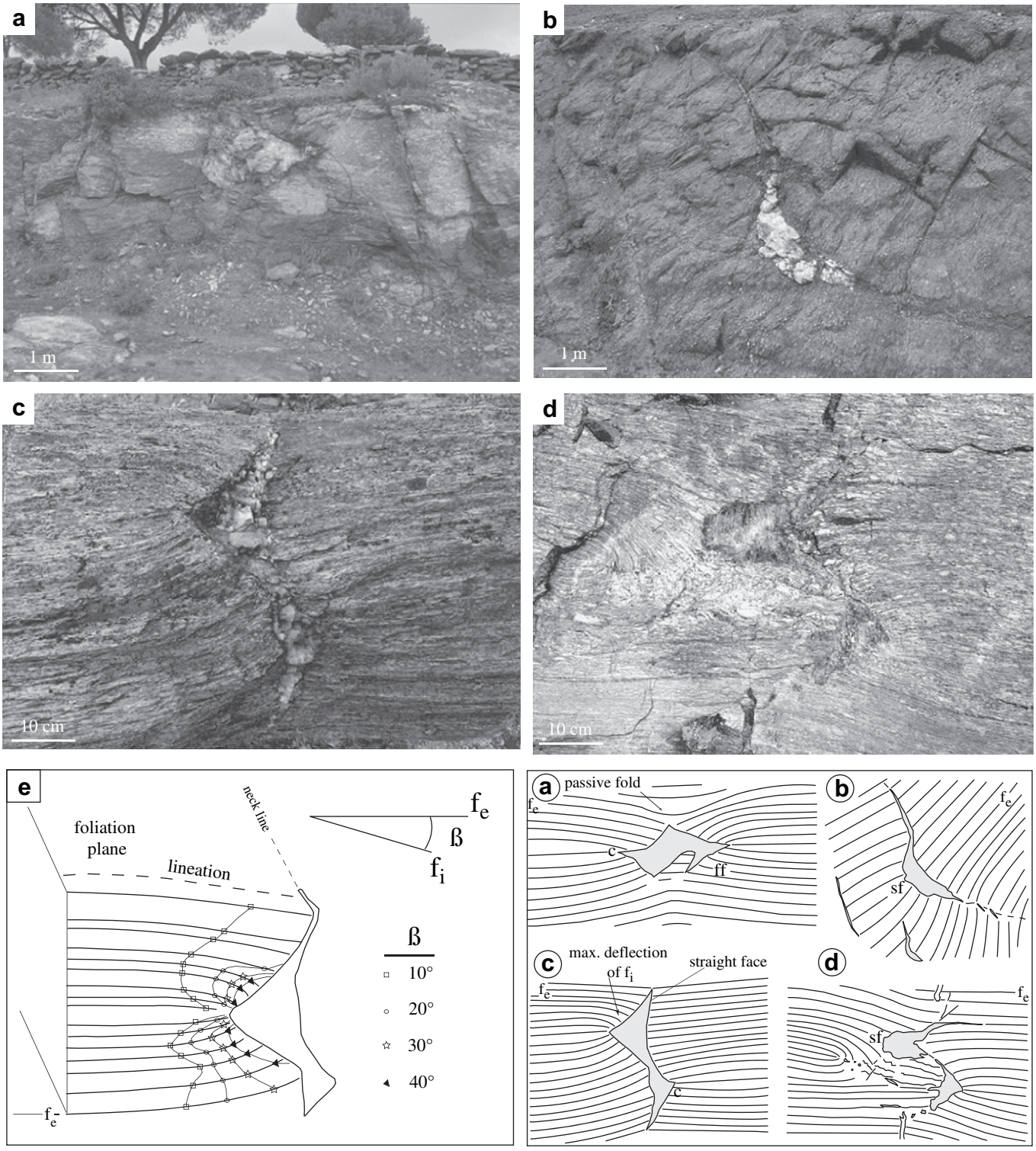

Fig. 5. Photographs and sketches (box at the lower right) of FBSs from the Çine Massif. All views are in cross-section normal to the boudin axis. (a) m-Scale lozenge-type FBS in orthogneiss, northwestern Çine Massif (location: 37°40′32N; 27°33′98E). Two symmetric cusps face in opposite direction and the foliation is deflected towards the central vein. (b) m-Scale asymmetric crescent-type FBS in orthogneiss, northeastern Çine Massif (location: 37°42′14N; 28°26′63E). Curved vein walls face the same direction. (c) X-type FBS in orthogneiss. Maximum deflection of foliation around veins is around cusps and the deflection angle decreases to the tips of the vein. On the opposite straight side of the vein foliation is at a high angle to the vein wall. Vein fill is biotite, quartz and feldspar (location: 37°42′36N; 28°27′69E). (d) cm-Scale double crescent-type FBS in orthogneiss, southern Çine Massif (location: 37°29′88N; 27°38′74E). This type has asymmetric double curved faces. (e) Contours connecting the same β angles measured along the foliation planes showing the deflection of foliation around cusp. Locations are shown in Fig. 2b.

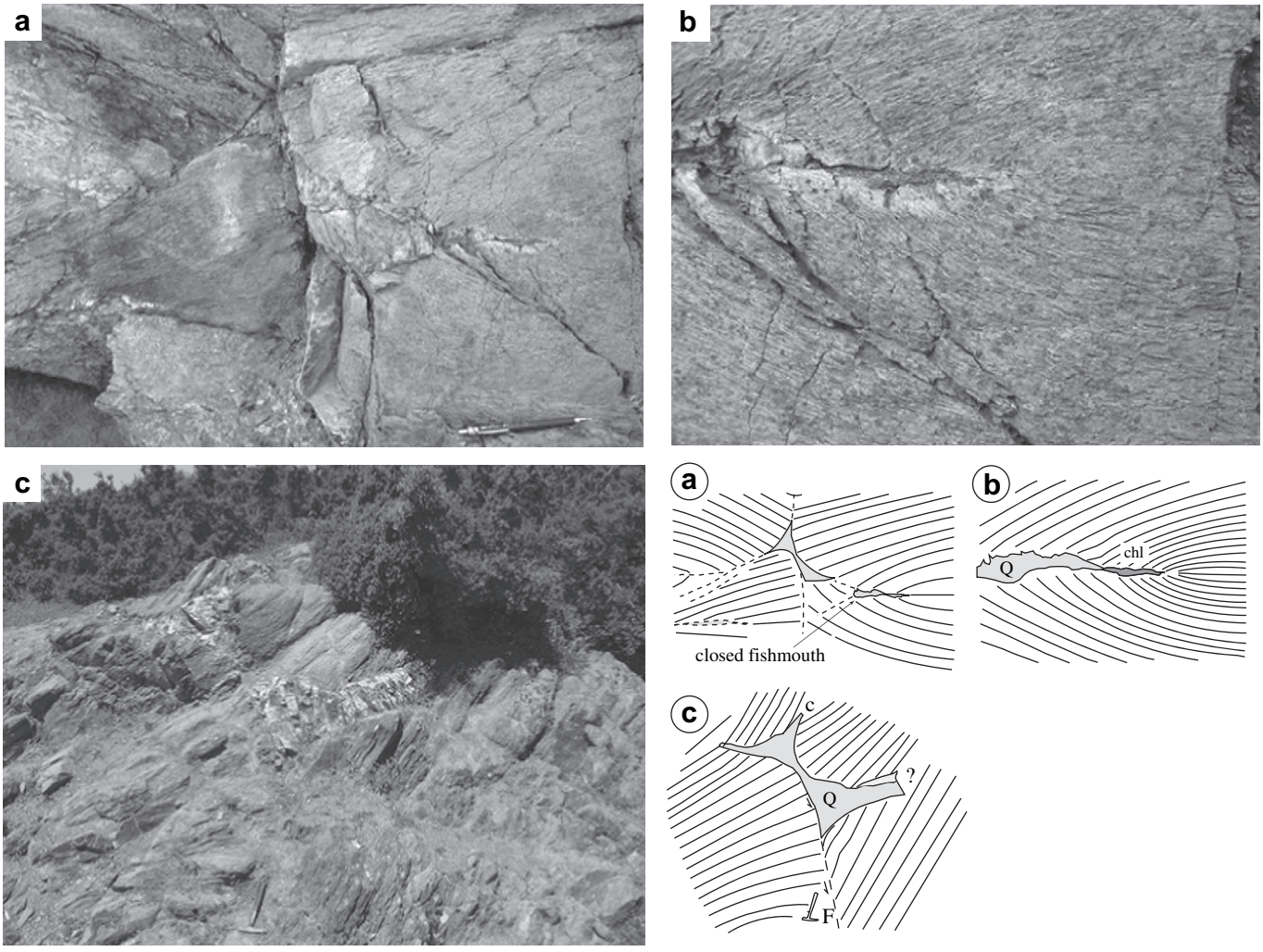

Fig. 6. Complex X-shaped FBSs from the northeastern Çine Massif. (a) X-type FBSs with closed fishmouth structure at the end of the cusps in metasediments of the Çine nappe (location: 37°47′37N; 28°22′44E). (b) Detail of closed fishmouth structure in (a). Note the alteration rim around the vein. (c) m-Scale X-type FBS in metasediments, northeastern Çine Massif (location: 37°47′37N; 28°22′71E). Note the asymmetric cusps and necking of foliation around the cusps. On the opposite sides from the cusps, where the vein wall is straight, foliation is at a high angle to the vein wall.

tips. Fishmouth structures can be found associated with all types of FBSs and form an end stage in the tightening of these structures.

The geometries described above are visible in cross-section parallel to the lineation in the rock, but the 3D shape of the FBS is not cylindrical. On foliation surfaces, FBSs occur mostly with one of two shapes; lens-shaped and triangular-shaped veins (Fig. 7). Both foliation and lineation bend symmetrically in on two sides of the lens-shaped veins (Fig. 7a). They belong to the symmetric FBS types described above. Around the triangular veins the lineation is straight and at a high angle to the vein contact on the straight face of the vein and on the opposite cusped side it is deflected (pinched in) in accord with the curved side of the vein but again at a high angle to the vein wall (Fig. 7b). Triangular veins belong to the asymmetric FBS types described in cross-sections. The curve of the cusp can be sharp, angular (e.g. X-type) or smooth (e.g. crescent- and double crescent-type) depending on the asymmetric FBS type. In the Çine Massif, FBS veins have a length/width ratio on the foliation surface of at least three and usually more.

3.1.1. Variations in geometry of FBSs in the Çine Massif

In strongly mylonitic rocks of the Selimiye shear zone in the southern Çine Massif, a number of interesting asymmetric types of boudinage structures have been found (Fig. 8). These local structures are small veins (Fig. 8a) in quartz micaschist and micaschist of the shear zone, which mainly developed in shearbands. In sections normal to the foliation and parallel to the aggregate lineation, these asymmetric types have lozenge-shaped and triangular quartz plugs in the neck region of FBSs and they differ in some aspects from the main common types mentioned above (Fig. 8). We therefore prefer to place them in another category.

Asymmetric lozenge-type FBSs have flanking folds on two opposite sides of the vein walls that are at a relatively high angle to the main foliation in the host rock. The foliation presents a shearband geometry on the other two sides of the vein,

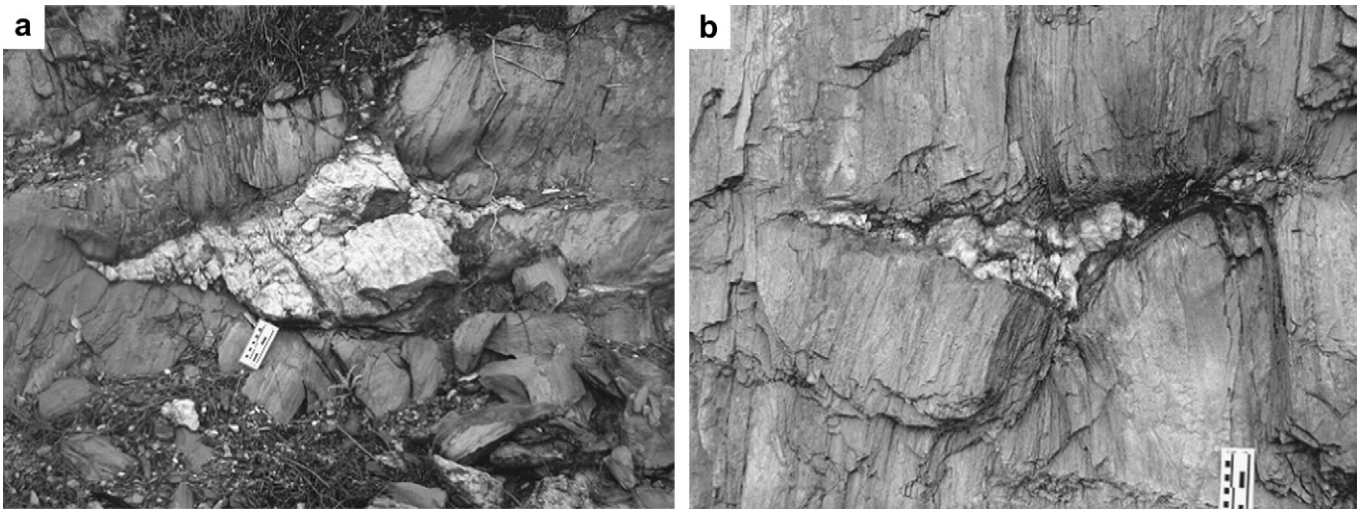

Fig. 7. Photographs of FBSs in cross-section looking down on the foliation plane. The aggregate lineation on foliation plane bends in towards the vein. (a) Symmetric FBS with a lens-shaped vein in the neck (location: 37°23′66N; 27°45′06E). (b) Asymmetric FBS with a triangular vein in the neck (location: 37°22′68N; 27°47′73E). Scale in the photographs is 10 cm long. Locations are shown in Fig. 2b.

where the vein walls lie at lower angles to the main foliation (Fig. 8b).

Relatively common are isolated triangular vein geometries (Fig. 8c–f), similar to those observed in X-type FBSs, but not occurring in pairs. These triangular veins show remarkable variety in their angular relations with the adjacent foliation in the host rock. Some types present asymmetric flanking folds on different faces of the triangle (Fig. 8c,d). In these types one face of the triangle is at a high angle or orthogonal to the main foliation in the host rock whereas the other two faces are oblique to the foliation. Such veins can be wing cracks, where fractures form and open at the tip of a fault (Fig. 8c), or cusped triangular veins that have one folded fracture wall (Fig. 8d). In the other types of FBSs with triangular neck veins (Fig. 8e,f), the foliation is symmetrically arranged on two sides of the vein. In such symmetrical triangular veins two faces of the triangular neck vein are oblique to the foliation and the angle between these two faces is acute. The other face of the triangle is parallel or at very low angle to the foliation.

Some FBSs in the Çine Massif are associated with a quartz layer in the central part of the boudin structure. These are not classical lithology-defined boudins, since the deflection of the foliation extends far beyond the width of the central quartz layer. However, the central quartz layer predates formation of the FBS and may play a role in localisation of boudinage in these structures.

3.1.2. Vein material

The boudin neck veins of FBSs in the Çine Massif are mostly filled with massive quartz in large single crystals and with spherulitic chlorite aggregates. Tourmaline, feldspar and biotite are also present in some veins in the studied areas. The veins can contain up to several cubic meters of quartz (Fig. 5). However, some FBSs have very little or no vein material in their cores, especially those that have a closed ‘‘fish-mouth’’ shape (Goscombe et al., 2004). Such FBS can be easily confused with isoclinal folds. Minerals in the veins are never fibrous or elongate in shape, but always coarse grained, equidimensional and blocky (Fig. 10a). This habit of the grains is an original feature of vein filling, and not due to deformation or recrystallisation; quartz in the veins is weakly deformed with some undulose extinction. Many veins contain facetted large quartz crystals that face a central void in the boudin necks.

In some outcrops in the gneisses (e.g. in the northeastern-most Çine Massif) spaced Mode I fractures cut the pervasive foliation, and are easily recognized by red-brown iron oxides. These Mode I fractures are mainly filled with chlorite and range in length from mm- to m-scale and are up to several mm wide. Wider fractures are mostly filled with massive quartz. In some cases biotite concentrations or stacks in the host rock are found at vein margins. Garnets in the host rock were altered to chlorite close to the veins.

Growth of minerals in narrow veins that open slowly leads to the formation of elongate or fibrous crystals (Bons, 2001; Hilgers et al., 2001). If veins open more rapidly than crystal growth, blocky crystals develop with faceted crystal faces according to their mineral-specific crystal morphology (Spry, 1969; Passchier and Trouw, 2005). The best examples of fibrous veins are found in low to medium grade rocks, while massive quartzo-feldspathic veins that must have filled tensile fractures are common at higher metamorphic grades (Etheridge et al., 1984). Extension fractures filled with minerals reflect the pressure–temperature conditions of their host rock.

The dominance of large facetted single quartz crystals and spherulitic chlorite in the veins in the FBSs of the Çine Massif suggest that the minerals did not grow by slow opening but grew into open fluid-filled space with a fluid pressure exceeding the minimum principal stress by at least the tensile strength of the rock. These fluid-filled voids must have been present for a substantial period of time during the later stages of deformation in the massif, while the FBSs developed; there

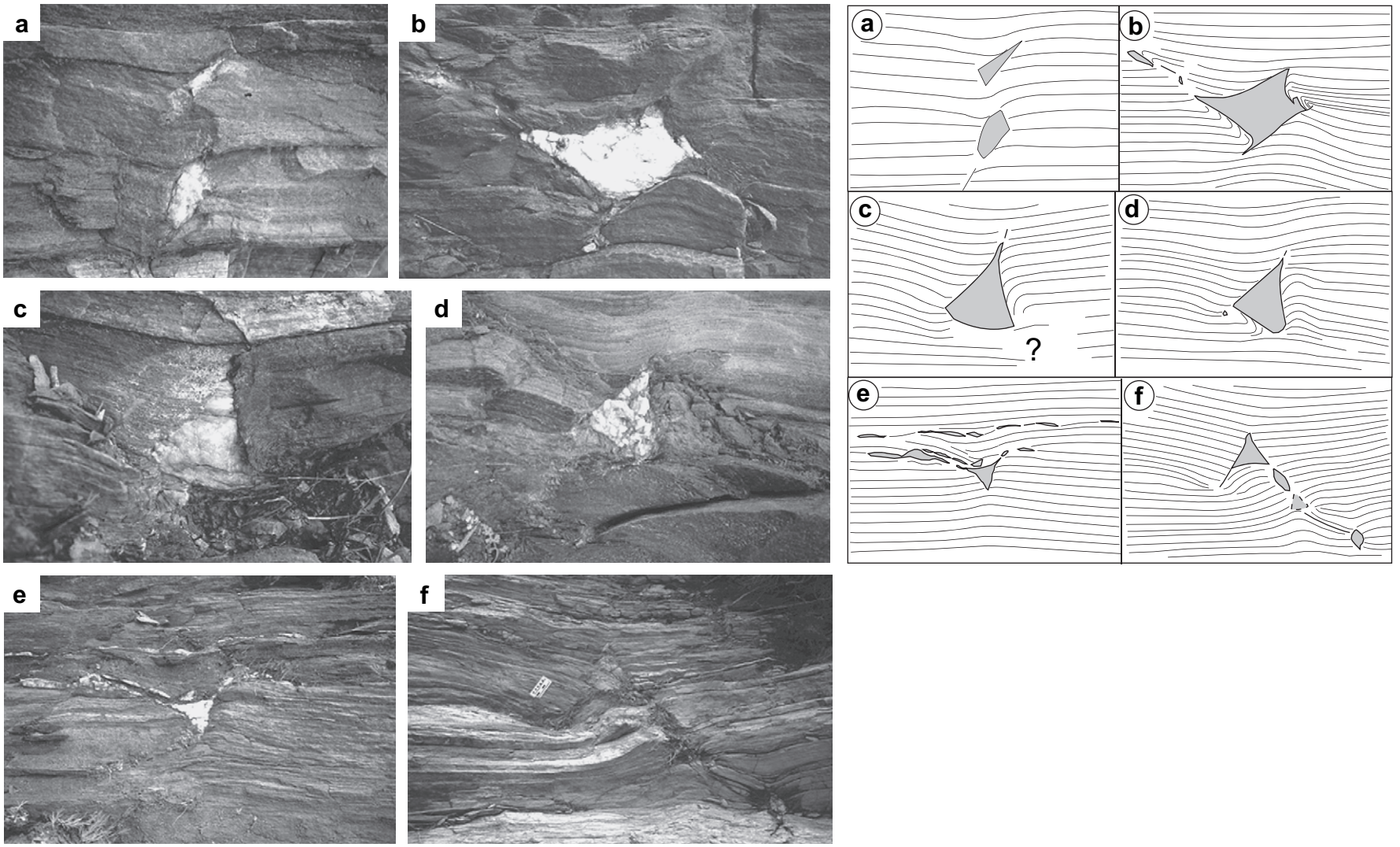

Fig. 8. Various types of FBSs with triangular veins from mylonitised quartz micaschist in the Selimiye shear zone, southern Çine Massif. (a) Small veins in a shearband. (b) Asymmetric lozenge-shaped vein with flanking folds on opposite sides of the vein walls that are at an angle to the main foliation in the host rock. On the upper left and the lower right sides of the vein foliation is deflected as in a shearband. (c) Triangular vein with asymmetric flanking folds, probably a type of wing crack. (d) Cusped triangular vein with flanking folds on both sides with small interlimb angles. (e) Triangular vein with fishmouth structure on the left side of the vein (location of outcrop for a–e: 37°22′74N; 27°47′82E). (f) Several triangular and lens-shaped veins in a shear zone with bending and passive amplification of foliation around and at the tips of the veins (location of outcrop: 37°28′61N; 27°35′19E). Locations are shown in Fig. 2b. The development of these variations of FBSs is explained in Fig. 14.

was time to allow first ductile deformation and infolding of fracture walls followed by vein filling, since the vein material is not deformed.

3.2. FBSs in Furka Pass–Urseren Zone

In order to test the general validity of our observations in gneiss and micaschist of the Çine Massif, we also studied FBSs in the Furka Pass–Urseren area of the central Alps.

In the Furka Pass–Urseren area a great number of FBSs occur, both symmetric and asymmetric (Fig. 3b). In general, the same types of FBSs are observed as in the Çine Massif. Closed fishmouth type lozenge-shaped FBSs dominate, many of which are asymmetric with flanking folds on one side (Fig. 9). The FBS neck veins are smaller than those of the Çine Massif, up to several tens of centimetres long. The associated neck veins are mostly lens-shaped. They are filled with coarse massive quartz, feldspar and spherulitic chlorite aggregates (Figs. 9 and 10b). Chlorite aggregates are not only found as vein fill but also occur along the edge of veins in the wall rock (Fig. 10b). Alteration rims in the host rock around boudin neck veins are common. They are easily recognized by

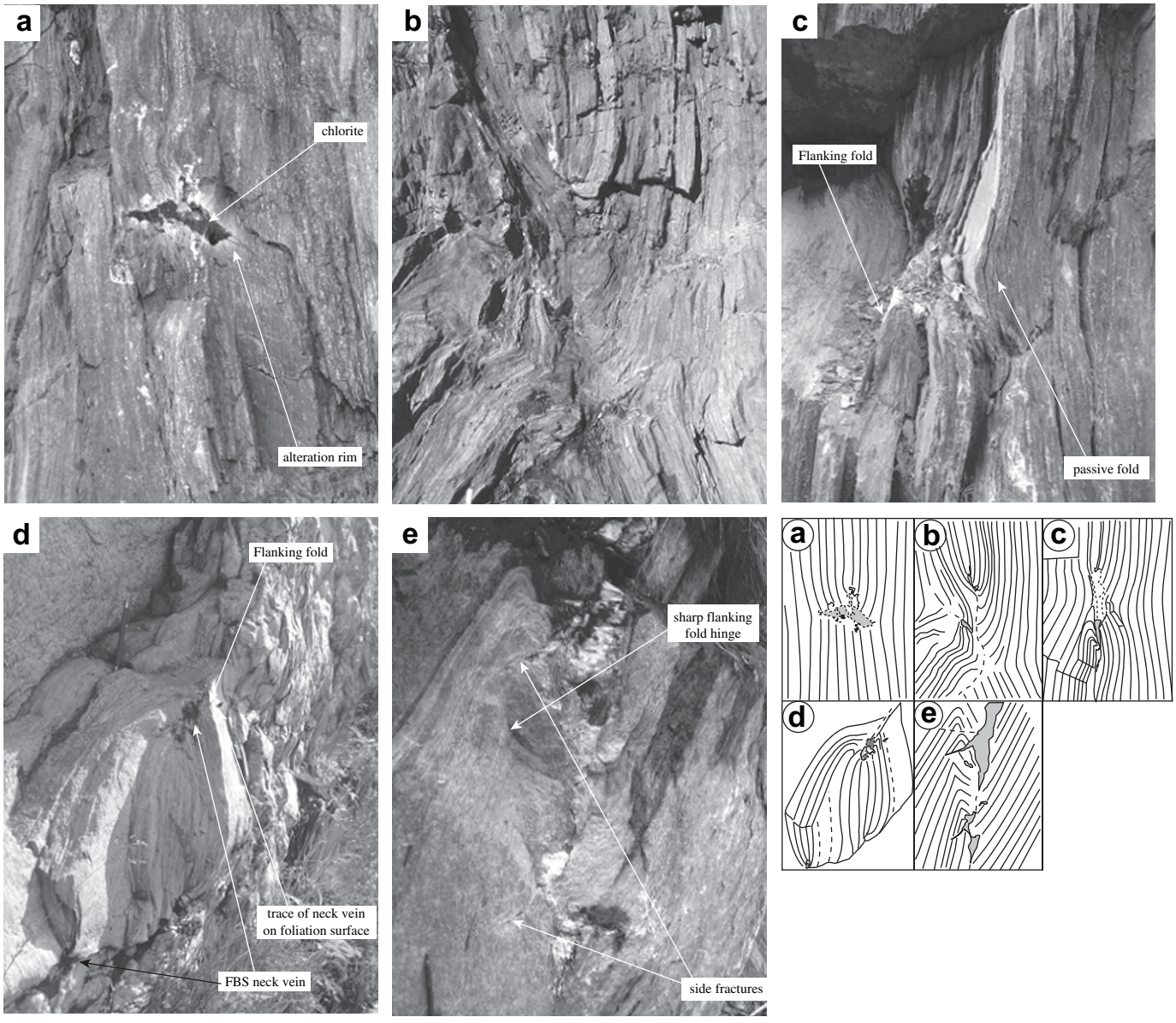

Fig. 9. Photographs and sketches of FBSs from the Furka Pass–Urseren Zone. All views are in cross-section normal to the FBS axis. (a) Symmetric FBS with alteration rim around a chlorite–quartz vein in mylonitic gneiss. (b) Asymmetric FBS with small quartz, feldspar, chlorite veins in boudin necks (location of outcrop for pictures a and b: 46°34′65N; 08°23′32E also indicated in Fig. 3b). (c) Asymmetric FBS, a neck vein lies parallel to the foliation and to the axial plane of a flanking fold with small interlimb angle in quartz–sericite schist. The open fold is due to passive amplification of foliation at the vein tip. (d) Boudin block between two neck veins filled with quartz, albite, chlorite and mica (location: 46°37′17N; 08°33′21E). (e) Central vein structure in a FBS neck pinched into several small lens-shaped veins. To the left of the veins are tight flanking folds with sharp hinges. Flanking folds are cut and slightly displaced by the small subsidiary fractures to the FBS neck (location: 46°37′11N; 08°33′05E).

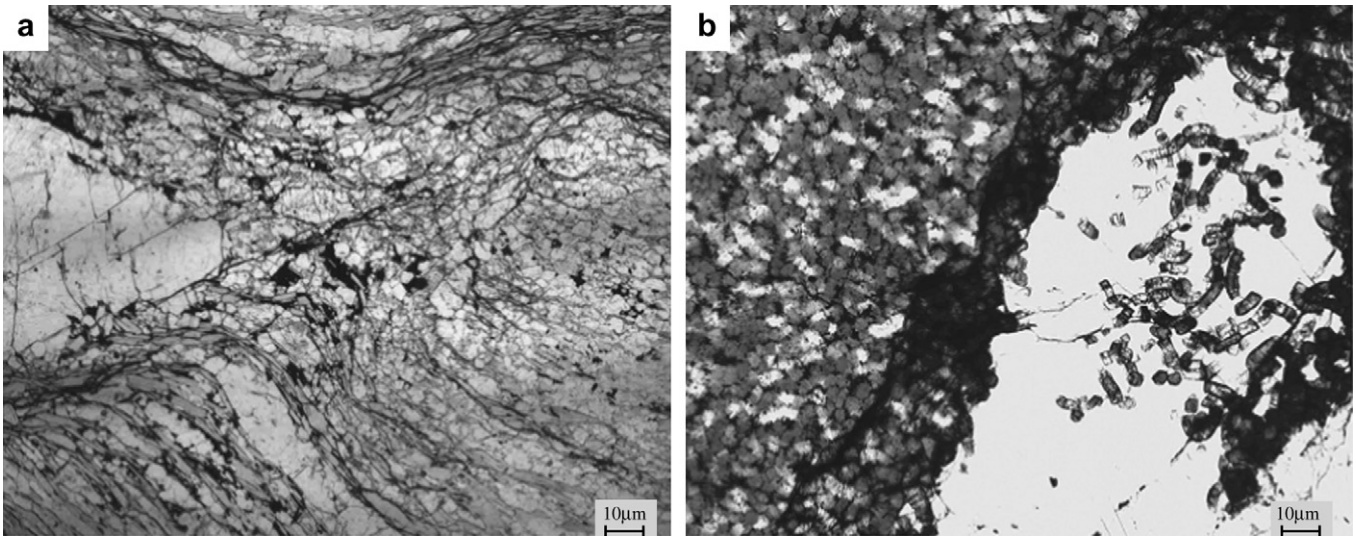

Fig. 10. Photomicrographs of FBS neck regions. (a) Fishmouth FBS. In the central part of the picture necking of the foliation in the host rock is visible close to the vein. The V-shaped vein in the FBS neck consists of massive blocky quartz. At the lower contact of the vein, micas (biotite + muscovite) bend in towards the vein as in a shearband (sample location: Labranda road, Çine Massif; 37°22′98N; 27°47′79E). (b) Spherulitic chlorite aggregates at the edge of and inside a feldspar filled neck vein (sample location: Belvedere, Furka Pass; 46°34′56N; 08°23′39E).

a difference in colour with the host rock (Fig. 9a), while their width depends on vein size.

On the foliation surface, FBS neck veins are lens-shaped with a high length/width ratio that exceeds 4. The local aggregate lineation is mostly at a high angle to the vein wall. However some late veins with lineation oblique to the vein wall are also found. In some outcrops, a crenulation is visible on micaceous foliation planes slightly oblique to the vein axes.

On planes normal to the foliation and parallel to the aggregate lineation FBS neck veins lie both highly oblique (Fig. 9a) and parallel to the foliation (Fig. 9b). They are present as a single vein or trains of several irregular lens-shape veins. Flanking folds adjacent to veins with axes parallel to the boudin axes (e.g. Fig. 9c) show interlimb angles changing from open to completely closed (Fig. 9). Gentle, open flanking folds are observed at FBSs where boudin neck veins are at a high angle to the foliation and are mostly associated with symmetric FBSs (Fig. 9a). Small interlimb angles of flanking folds, mostly less than 30° where fold limbs became almost parallel to each other and to the vein wall, are observed with veins parallel or at low angle to the foliation and near asymmetric FBSs (Fig. 9b–e). In some cases flanking folds are cut by minor fractures or small veins at a high angle to the FBS neck, probably formed as accommodation fractures in response to a high angle of rotation of the vein (Fig. 9e). The curvature of the flanking folds is strongest on one side of the FBS neck region (Fig. 9b–e). On the opposite side of the vein the foliation is parallel or at a low angle to the vein wall. Although rare, foliation boudins separated by two veins have been found in the Urseren area (Fig. 9d). Mode I and/or conjugate mineral-filled fractures with high aspect ratio are also observed at high angles to the foliation but these are probably late, based on cross-cutting relations seen in outcrop. In some outcrops FBSs are cut along the neck region and displaced by cm- to m-scale faults or shear zones that lie at an angle to the main foliation in the host rock (Fig. 3b).

The rocks of the Çine nappe contain a subhorizontal foliation and lineation developed at upper amphibolite to greenschist facies conditions, while the rocks in the Furka Pass–Urseren Zone present vertical to subvertical foliation and lineation formed under greenschist facies. The closed fishmouth type lozenge-shaped FBSs, which dominate here (Fig. 9b,c) are thought to be the end-stages in development of more open asymmetric lozenge-type veins by a process similar to that in the Çine Massif.

4. Numerical modelling

In order to explain the geometry of the developing foliation boudinage structures, we carried out simple numerical experiments using FLAC (Itasca Consulting Group, Inc., 1998) described in Passchier and Druguet (2002). FLAC is a 2D explicit finite difference model and is based on 4-node quadrilateral meshes.

In all numerical experiments we used a grid size of 60×42 elements in x- and y-coordinates, respectively. The exact location of each element and each node in the grid, in which all variables are stored, is defined by a pair of x-, y-coordinates. Fractures were modelled by removing elements and replacing them by a void within a finite difference mesh (Figs. 11 and 12). Experiments were run for a range of kinematic vorticity numbers from pure shear to simple shear in several combinations with different initial fracture orientations (Figs. 11 and 12), θ varying between 30° and 150°. Here, only the most important results are shown. We adopted a visco-elastic (Maxwell) substance model in numerical simulations. Kinematics of flow in the models was defined as a function of the bulk-stretching rate, which was set at $1e-10\ s^{-1}$, and the

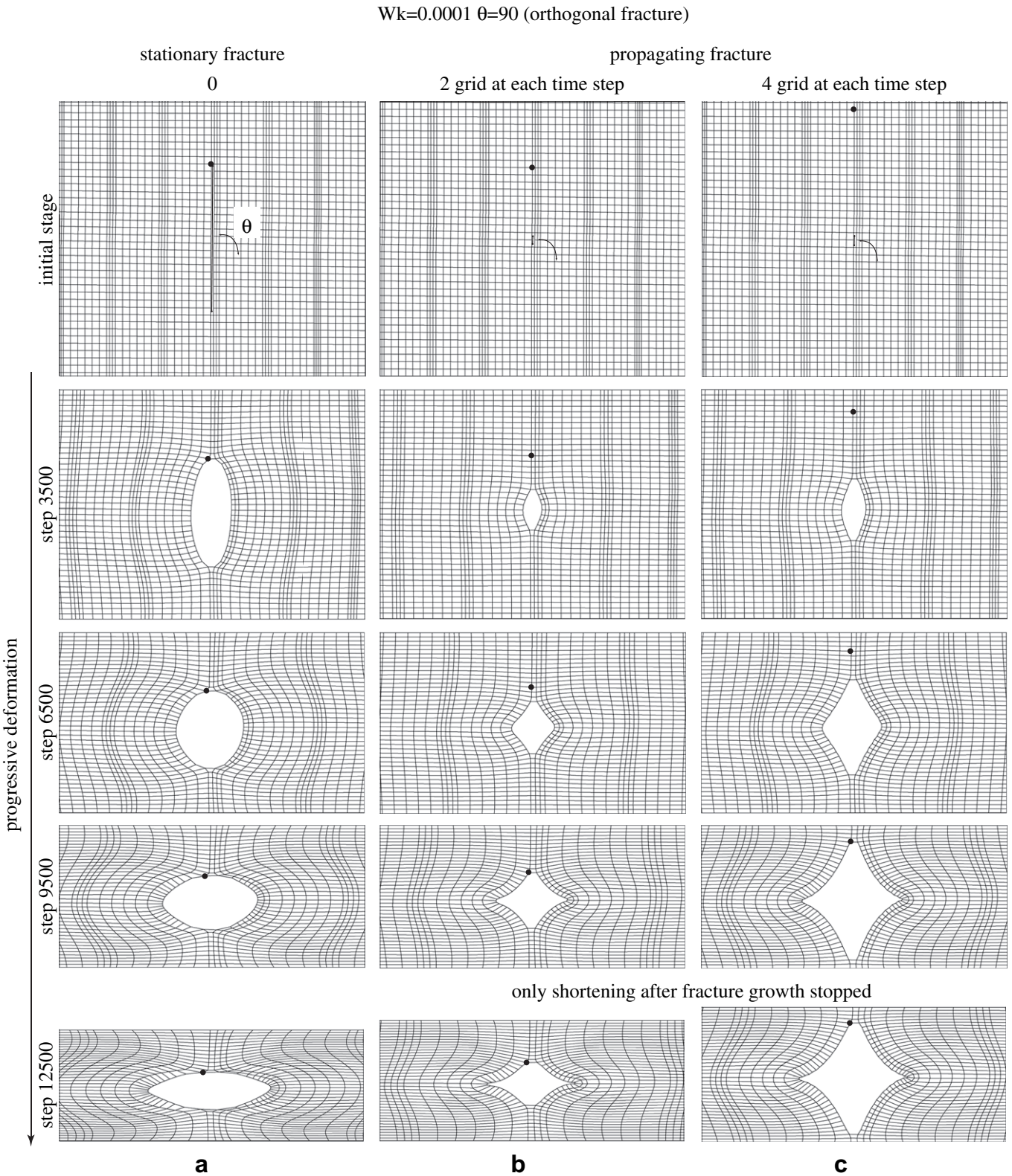

Fig. 11. Results of FLAC experiments showing the effect of different fracture propagation speeds on necking and vein geometry during ductile flow. Only the central part of the grid in the models is shown. In the models grids were deformed under pure shear conditions and $\theta = 90^{\circ}$. θ is an angle between the initial fracture and the horizontal grid-foliation. Initial geometry is shown in the first row, results of deformation experiments in the following rows. (a) Absence of fracture growth during deformation leads to elliptical veins with strong ductile deformation at the fracture tips. (b, c) Fracture propagation during deformation leads to veins with a lozenge shape similar to those observed in most foliation boudinage structures. The last row (at step 12,500) shows the structures at stages where further deformation has accumulated after fracture growth was stopped. With slow fracture propagation, cusps are more pronounced and lozenge geometries more angular. A small black dot is fixed on one node in the grid to show the displacement throughout the progressive deformation in the experiments.

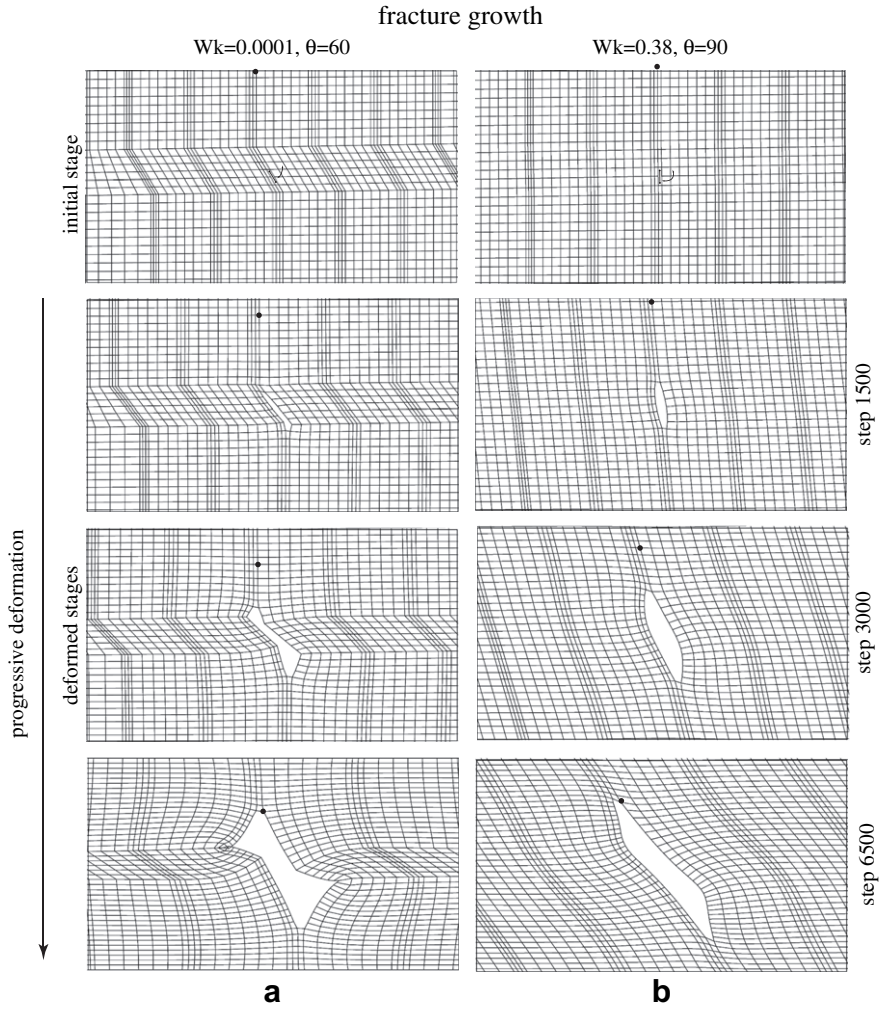

Fig. 12. Examples of FLAC experiments performed for asymmetric fracture geometry. The initial stages are shown in the first row. In the lower rows both examples have fracture propagation during ductile flow. (a) Initial oblique fracture ($\theta = 60^\circ$) deformed in pure shear ($W_k = 0.0001$). (b) Initial orthogonal fracture deformed in simple shear ($W_k = 0.38$). Deformed stages in the lower rows show the development of asymmetric FBS, opening of a neck vein and asymmetric necking in the adjacent grid. Flanking structures form due to flow partitioning around fractures and opening veins. The geometry of the internal foliation is similar to that observed in field examples of X-type veins.

kinematic vorticity number (W_k), ranging between 0 (pure shear) and 1 (simple shear). The maximum creep time was set to 8e8 s. Material properties were set as follows: bulk modulus = 2e10 Pa, shear modulus = 1.2e10 Pa, viscosity = 1e19 Pa s and Poisson's ratio = 0.25.

The experiments were run for 6500–12,500 steps. Elements were removed from the mesh at each 1000 (Fig. 11b,c) or 500 steps (Fig. 12) to mimic fracture propagation. We examined fracture growth and deformation for experiments run at different rates and the processes in individual experiments at each stage. The plots in Figs. 11 and 12 are shown at the same deformation steps for each experiment. Aspect ratios of initial fractures were defined as 21:1 for a stationary fracture (Fig. 11a) and 2:1 in fracture growth experiments (Figs. 11b,c and 12) as the ratio of a number of elements removed in vertical (y) direction to the elements removed in horizontal (x) direction. Models assume an initial fracture that can remain open during the deformation. We simulated fracture growth by alternating deformation steps with steps where we allowed removal of grid elements at the tip of the initial fracture. Although the method to simulate a fracture is rather simple and without feedback between fracture shape, stress intensity and fracturing, it gives interesting results.

One important observation is that if an open fracture precedes ductile deformation in the rock and is fixed in length and the surrounding material is deformed in pure shear, the fracture opens to an elliptical and even circular shape (Fig. 11a). Only if we allow fractures to grow laterally during ductile deformation of the wall rock, a typical lozenge shape forms and the walls of the vein start to buckle towards a fish-mouth shape (Fig. 11b,c). The rounded, lens-shaped opening that occurs for non-propagating fractures was never observed in natural FBSs. Short veins with slightly convex shape are common in nature, also in the Çine and Furka areas, and these may in some cases represent incipient FBSs. From our field observations and the FLAC experiments it seems, however, that fractures must grow laterally during opening to give the typical lozenge shape that is characteristic for many FBSs.

The initial orientation of the fracture is important in defining the resulting geometries through progressive deformation. Fig. 12a shows an example of the development of asymmetric FBS in which an initial oblique fracture ($\theta = 60°$) propagates and is deformed under pure shear conditions. During progressive deformation, rotation of and slip along the fracture lead to opening of an asymmetric vein and development of flanking structures in the adjacent grid. Similar asymmetric FBSs are also developed in simple shear (Fig. 12b). However, angular relations between the adjacent grid and the vein are slightly different from those in Fig. 12a. The simple shear experiment was carried out with a vertical initial fracture. The asymmetry could be expected to be even greater with an inclined initial fracture parallel to the instantaneous shortening direction of simple shear. In FLAC it is not possible to model this geometry because vein walls can overlap since non-connected elements in the model do not register each other.

5. Development of foliation boudinage structures (FBSs)

Foliation boudinage structures form by a combination of ductile deformation (indicated by the deflection and folding of foliation in the rock), brittle fracturing and deposition of vein material. The large variety in vein shapes, from disc-shaped veins through massive lozenge-shaped veins containing cubic meters of quartz to fishmouth boudin structures, shows that vein filling from aqueous solution can happen at all stages of the formation process of FBSs. We assume from field observations and FLAC experiments that the sequence disc-, lozenge- to fishmouth shapes represent a series of increasing deformation intensity, and that each category represents early stages of arrested deformation and vein deposition. Since quartz filling of boudin veins is rarely deformed or recrystallised, lozenge and fishmouth boudins must form before veins are filled, e.g. when the boudin veins were open, water-filled cavities. Since some of them contain cubic meters of quartz, cavities of this size can apparently open during ductile deformation of gneiss and micaschist at greenschist to amphibolite facies conditions. This may have interesting consequences for volumes of stored fluid and patterns of fluid migration in metamorphic rocks.

Completely closed fishmouth veins, as observed in the Furka area, probably also form by closure of open fluid-filled voids. The fact that these structures are more common in the Furka area than in the Çine Massif can be an effect of the higher ductile strain in the Furka area and the different rock types. Theoretically, closed fishmouth structures could also form by dissolution of material in more open lozenge-shaped veins. However, we did not find any evidence for such a mechanism such as deformation in the veins, stylolites or enrichment of insoluble material on vein edges or in the veins.

The presence of brittle fractures at low to medium metamorphic grade implies that fluid pressure must have been lithostatic. Although the name ‘‘foliation boudinage’’ implies that such structures can only form in foliated rock, e.g. due to its mechanical anisotropy, we find that the best foliation boudins are actually formed in weakly foliated gneiss rather than in strongly foliated micaschist or mylonite. Apparently, fluid pressure is more critical than fabric strength, although the fabric may play a role in determining the orientation of fractures. Therefore, the name ‘‘foliation boudin’’ is actually misleading.

5.1. Development of the main types of FBSs

Under pure shear condition layer normal shortening and foliation-parallel extension can cause the development of Mode I fractures if fluid pressure in the rock is high (Figs. 13 and 14). During further progressive deformation, the fractures can open and develop a lens or lozenge shape. If associated minor faults occur along the foliation planes, triangular veins can form in pure shear (Figs. 8e,f, 13 and 14). FLAC experiments indicate

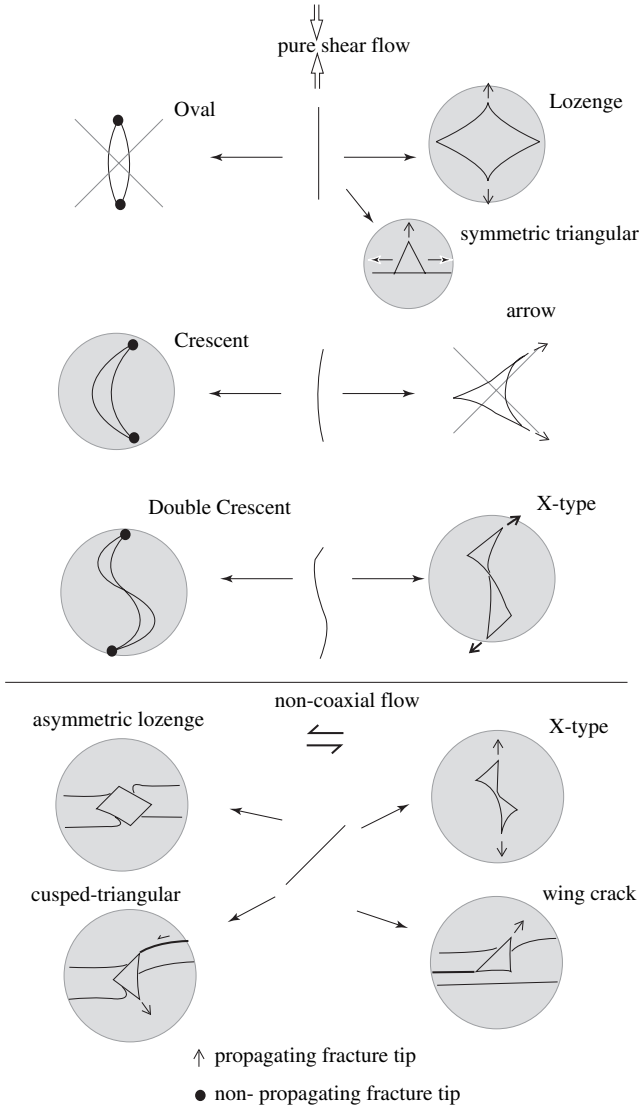

Fig. 13. Schematic presentation of the types of veins that can develop in FBSs depending on shape of the initial fracture, fracture propagation and bulk flow. Straight fractures will tend to propagate and form lozenge-, triangular- or X-type veins, while curved ones may fold and deform into crescent-type veins. Shapes in grey circles occur in nature. Crossed out shapes have not been observed. See text for further explanation.

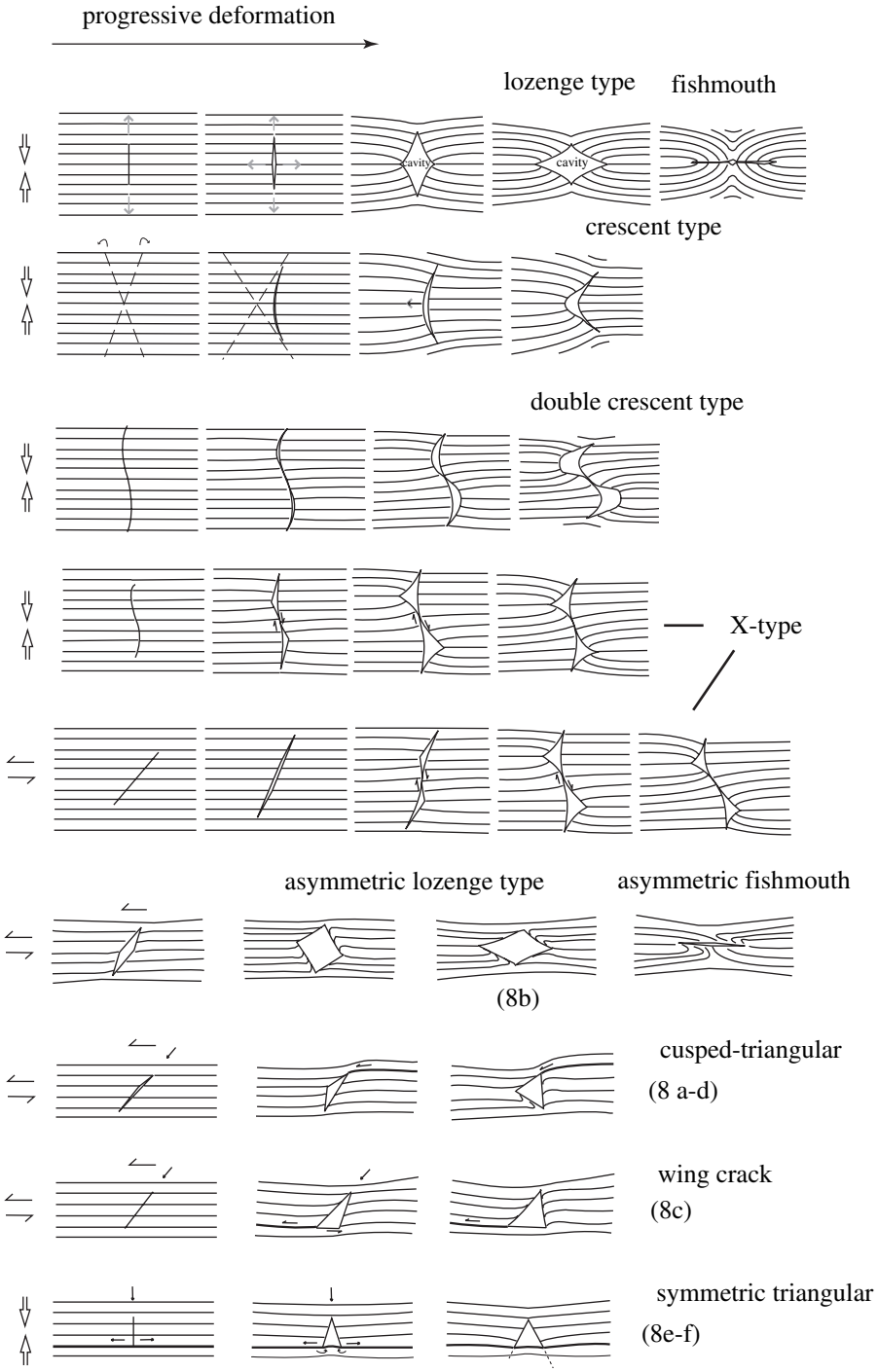

Fig. 14. Inferred development mechanisms of observed FBSs. Different vein geometries can form depending on flow type, fracture propagation, fracture rotation or folding, and combinations of these. See text for further explanation.

that lens-shaped veins form in the case of non-propagating fractures, while lozenge-shaped ones form when Mode I fractures propagate. The reason is probably that propagating Mode I fractures cause the tip sections of the fracture walls to rotate outwards passively, remaining relatively straight and concentrating most ductile deformation in cusps in the centre of the fracture walls. If a fracture does not propagate, the walls deform more uniformly. This model seems to be supported by the observation that lens-shaped fractures in FBSs are narrow and have only been observed if FBSs are weakly developed. Wide-lens-shaped veins do form in necks of boudinaged layers in other areas, but this may be due to lack of propagation of fractures beyond the affected layer.

Rotation of fracture walls leads to development of flanking structures around veins; since the fracture walls are bound by fluid on one side, they must be planes of zero shear stress, and can only support shortening or extension in that direction. In the far field, this does not apply and the resulting difference

in the orientation of the stress field will lead to development of flanking folds in foliation boudins (Fig. 14).

Several types of symmetric and more or less closed lozenge-shaped FBSs can form depending on when vein filling occurs. If no vein filling occurs, closed fishmouth shapes form. Lozenge-shaped FBS veins only form in pure shear if both limbs of the former fracture bend outwards (Fig. 14). Crescent-type veins are interesting because they have two vein walls that curve in the same direction. They probably form if fractures are initially not straight, for example because the rock is inhomogeneous or because fracturing does not occur in tension, but in shear due to relatively high differential stress (Mode II fractures). If an initial fracture is curved, both fracture walls may curve out in the direction of the initial bend in the fracture. An alternative is that an initial Mode I fracture is folded into an open crescent shape before it starts opening. Theoretically, one would expect that such curved fractures could lead to triangular, arrow shaped veins like half lozenge-shaped veins, with only one cusp (Fig. 13). In fact, the triangular veins that we found have other geometries and do not seem to form in this way (Fig. 14). Instead, crescent-shaped veins form that have the smooth geometry of disc-shaped veins. The reason may be that if fracture walls bend out in two directions, the separating walls cause enhanced tension in the fracture tip and outward fracture propagation; if both walls curve in the same direction, such tension is less pronounced and fractures may not propagate outward at all, forming smooth curving veins instead (Fig. 13).

If a fracture forms in non-coaxial flow, it will rotate with progressive deformation and a slip component will develop along the open fracture; this will lead to asymmetric outward bulging on both sides of the fracture, and ultimately to X-shaped veins if the fracture continues to propagate (Fig. 14). Possibly, X-shaped veins can also form if the rock is heterogeneous and initial cusps do not develop opposite (Figs. 13 and 14). If lozenge-shaped veins develop in non-coaxial flow, different types of flanking folds will develop on both sides, and asymmetric lozenge-shaped veins or asymmetric fishmouth FBSs can form. Double crescent veins may form as a special type of X-veins where the fault tips do not propagate; alternatively, they could form in coaxial flow if a fracture has originally a double curvature, or if it is folded into two opposite-facing folds before it starts opening.

Summarising, Fig. 13 shows the types of veins that could theoretically form out of straight or curved veins in pure shear and non-coaxial flow. Those in grey circles are the ones that we actually observed, while oval and arrow veins may not develop in natural FBSs for reasons given above. Fig. 14 shows the envisioned models for development of each of the observed types of FBSs.

5.2. Development of other varieties of structures in the Selimiye shear zone

Some types of mostly triangular FBSs are only found in the metasediments of the Çine Massif in the Selimiye shear zone and are not observed at all in the orthogneisses with coarser fabric. We suggest that they are restricted to micaschists in the shear zone and that strong anisotropy planes defined by micas, which provide easy slip planes, play an important role in their development (Fig. 14). After the development of a set of fractures at high fluid pressures in the shear zone, the stress field around the fractures changes. Combination of slip along the fractures and rotation leads to opening of the neck veins and development of various flanking structures around them (Fig. 14).

6. Conclusions

From our observations of natural examples in the studied areas four main types of foliation boudinage structures can be distinguished; lozenge-, crescent-, double crescent- and X-type. All these types occur as open, vein filled structures but also show transition to a fishmouth geometry.

Foliation boudinage structures form by ductile deformation adjacent to brittle fractures and open fluid-filled cavities in metamorphic rocks. Fluid pressure in the rock must be high in order to form foliation boudinage, and seems to be a more important factor to determine whether foliation boudinage will form than the actual presence of a strong planar anisotropy. As such, the term foliation boudinage may be misleading.

The geometry of foliation boudinage structures depends on the shape of the central vein and deflection of foliation close to this vein into flanking folds. The shape of the boudin neck veins in foliation boudinage depends on the initial orientation and shape of the fracture, the propagation behaviour of the fracture, the geometry of bulk flow, and the stage at which mineral filling takes place. FLAC experiments show that fracture propagation during ductile deformation strongly influences the geometry of developing veins. The cusps of the veins are better developed and more pronounced in the case of propagating fractures.

The geometry of deflected foliation in flanking folds is directly related to the shape of the veins, since the deflection is due to the fact that the veins are originally open fluid-filled cavities; as a result, principal stress axes must be parallel and orthogonal to vein walls and this defines the geometry of ductile flow close to the veins. Flanking folds will therefore develop during further progressive ductile deformation due to the difference in orientation of the stress field close to open veins and in the far field. The four main types of foliation boudinage described in this paper can be explained by an interplay of these factors. Complete collapse of non-mineral-filled open cavities formed by foliation boudinage allows the formation of closed fishmouth structures.

Acknowledgements

Constructive reviews by Ben Goscombe and Paul F. Williams are gratefully acknowledged. We thank Talip Güngör and Hermann Lebit for their help and company in the study

areas. This project was funded by the DFG-Graduiertenkolleg ''Composition and Evolution of Crust and Mantle''.

References

Albrecht, J., Biino, G.G., Mercolli, I., Stille, P., 1991. Mafic–ultramafic rock associations in the Aar, Gotthard and Tavetsch massifs of the Helvetic domain in the Central Swiss Alps: markers of ophiolitic pre-Variscan sutures, reworked by polymetamorphic events? Schweizerische Mineralogische und Petrographische Mitteilungen 71, 295–300.

Albrecht, J., 1994. Geologic units of the Aar Massif and their pre-Alpine rock associations: a critical review. Schweizerische Mineralogische und Petrographische Mitteilungen 74, 5–27.

Aerden, D.G.A.M., 1991. Foliation-boudinage control on the formation of the Rosebery Pb–Zn orebody, Tasmania. Journal of Structural Geology 13 (7), 759–775.

Bernoulli, D., Graciansky, P.C.D., Monod, O., 1974. The extension of the Lycian nappes (SW Turkey) into the southeastern Aegean islands. Eclogae Geologicae Helvetiae 67, 39–90.

Bons, P., 2001. Development of crystal morphology during unitaxial growth in a progressively widening vein: I. The numerical model. Journal of Structural Geology 23, 865–872.

Bozkurt, E., Satır, M., 2000. The southern Menderes Massif (western Turkey): geochronology and exhumation history. Geological Journal 35, 285–296.

Bozkurt, E., 2004. Granitoid rocks of the southern Menderes Massif (southwestern Turkey): field evidence for Tertiary magmatism in an extensional shear zone. International Journal of Earth Sciences 93, 52–71.

Bozkurt, E., Winchester, J.A., Mittwede, S.K., Ottley, C.J., 2006. Geochemistry and tectonic implications of leucogranites and tourmalines of the southern Menderes Massif, Southwest Turkey. Geodinamica Acta 19, 363–390.

Bozkurt, E., 2007. Extensional v. contractional origin for the southern Menderes shear zone, SW Turkey: tectonic and metamorphic implications. Geological Magazine 144, 191–210.

Candan, O., Dora, O.Ö., 1997. The generalized map of the Menderes Massif. Department of Geological Engineering, Dokuz Eylül University, Izmir.

Candan, O., Dora, O.Ö., Oberhänsli, R., Oelsner, F., Dürr, S., 1997. Blueschist relicts in the Mesozoic cover series of the Menderes Massif and correlations with Samos Island, Cyclades. Schweizerische Mineralogische und Petrographische Mitteilungen 77, 95–99.

Cobbold, P.R., Cosgrove, J.W., Summers, J.M., 1971. Development of internal structures in deformed anisotropic rocks. Tectonophysics 12, 23–53.

Druguet, E., Carreras, J., 2006. Analogue modelling of syntectonic leucosomes in migmatitic schists. Journal of Structural Geology 28, 1734–1747.

Erdogan, B., Güngör, T., 2004. The problem of the core–cover boundary of the Menderes Massif and an emplacement mechanism for regionally extensive gneissic granites, western Anatolia (Turkey). Turkish Journal of Earth Sciences 13, 15–36.

Etheridge, M.A., Wall, V.J., Cox, S.F., 1984. High fluid pressures during regional metamorphism and deformation: implications for mass transport and deformation mechanism. Journal of Geophysical Research 89 (B6), 4344–4358.

Frey, M., Mahlmann, R.F., 1999. The Alpine metamorphism of the central Alps. Schweizerische Mineralogische und Petrographische Mitteilungen 79, 135–154.

Gessner, K., 2000. Eocene Nappe Tectonics and Late-Alpine Extension in the Central Anatolide Belt, Western Turkey – Structure, Kinematics and Deformation History. PhD thesis, University of Mainz, Germany.

Gessner, K., Piazolo, S., Güngör, T., Ring, U., Kröner, A., Passchier, C.W., 2001. Tectonic significance of deformation patterns in granitoid rocks of the Menderes nappes, Anatolide belt, southwest Turkey. International Journal of Earth Sciences 89, 766–780.

Gessner, K., Collins, A.S., Ring, U., Güngör, T., 2004. Structural and thermal history of poly-orogenic basement: U–Pb geochronology of granitoid rocks in the southern Menderes Massif, western Turkey. Journal of the Geological Society (London) 161, 93–101.

Goscombe, B.D., Passchier, C.W., 2003. Asymmetric boudins as shear sense indicators – an assessment from field data. Journal of Structural Geology 25, 575–589.

Goscombe, B.D., Passchier, C.W., Hand, M., 2004. Boudinage classification: end-member boudin types and modified boudin structures. Journal of Structural Geology 26, 739–763.

Graciansky, P.Ch.de, 1968. Teke Yarımadası (Likya) Toroslarının üst üste gelmis ünitelerinin stratigrafisi ve Dinaro-Toroslar'daki yeri. MTA Dergisi 71, 73–93.

Grasemann, B., Stüwe, K., 2001. The development of flanking folds during simple shear and their use as kinematic indicators. Journal of Structural Geology 23, 715–724.

Grasemann, B., Stüwe, K., Vannay, J.C., 2003. Sense and non-sense of shear in flanking structures. Journal of Structural Geology 25, 19–34.

Güngör, T., 1998. Stratigraphy and tectonic evolution of the Menderes Massif in the Söke-Selçuk Region. PhD thesis, Dokuz Eylül University, Izmir.

Hambrey, M.J., Milnes, A.G., 1975. Boudinage in glacier ice – some examples. Journal of Glaciology 14, 383–393.

Hanmer, S., 1986. Asymmetrical pull-aparts and foliation fish as kinematic indicators. Journal of Structural Geology 8, 111–122.

Hetzel, R., Reischmann, T., 1996. Intrusion age of Pan-African augen gneisses in the southern Menderes Massif and the age of cooling after Alpine ductile extensional deformation. Geological Magazine 133, 565–572.

Hilgers, C., Koehn, D., Bons, P.D., Urai, J.L., 2001. Development of crystal morphology during unitaxial growth in a progressively widening vein: II. Numerical simulations of the evolution of antitaxial fibrous veins. Journal of Structural Geology 23, 873–885.

Itasca Consulting Group, Inc., 1998. FLAC: Fast Lagrangian Analysis of Continua, Version 3.40. Itasca Consulting Group, Inc., Minneapolis, MN, USA.

Kröner, A., Sengör, A.M.C., 1990. Archean and Proterozoic ancestry in late Precambrian to early Paleozoic crustal elements of southern Turkey as revealed by single-zircon dating. Geology 18, 1186–1190.

Lacassin, R., 1988. Large-scale foliation boudinage in gneisses. Journal of Structural Geology 10, 643–647.

Lebit, H., 1989. Die Urserenzone zwischen Realp und Tiefenbach (Kanton Uri/Schweiz). Unpublished Diplomarbeit, Freiburg.

Lloyd, G.E., Ferguson, C.C., 1981. Boudinage structure: some new interpretations based on elastic–plastic finite element simulations. Journal of Structural Geology 3, 117–128.

Lloyd, G.E., Ferguson, C.C., Reading, K., 1982. A stress-transfer model for the development of extension fracture boudinage. Journal of Structural Geology 4, 355–372.

Loos, S., Reischmann, T., 1999. The evolution of the southern Menderes Massif in SW Turkey as revealed by zircon dating. Journal of the Geological Society (London) 156, 1021–1030.

Marquer, D., Burkhard, M., 1992. Fluid circulation, progressive deformation and mass-transfer processes in the upper crust: the example of basement–cover relationships in the external crystalline massifs, Switzerland. Journal of Structural Geology 14, 1047–1057.

Milnes, A.G., Pfiffner, O.A., 1977. Structural development of the Infrahelvetic complex, eastern Switzerland. Eclogae Geologicae Helvetiae 70, 83–95.

Platt, J.P., Vissers, R.L.M., 1980. Extensional structures in anisotropic rocks. Journal of Structural Geology 2, 397–410.

Passchier, C.W., 2001. Flanking structures. Journal of Structural Geology 23, 951–962.

Passchier, C.W., Druguet, E., 2002. Numerical modelling of asymmetric boudinage. Journal of Structural Geology 24, 1789–1803.

Passchier, C.W., Trouw, R.A.J., 2005. Microtectonics, second ed. Springer-Verlag, Berlin, 366 pp.

Ramberg, H., 1955. Natural and experimental boudinage and pinch- and swell structures. Journal of Geology 63, 512–526.

Ramsay, J.G., Huber, M.I., 1983. The Techniques of modern structural geology. In: Strain Analysis, vol. 1. Academic Press, London, 307 pp.

von Raumer, J., Albrecht, J., Bussy, F., Lombardo, B., Ménot, R.-P., Schaltegger, U., 1999. The Palaeozoic metamorphic evolution of the Alpine external massifs. Schweizerische Mineralogische und Petrographische Mitteilungen 79, 5–22.

Régnier, J.L., Ring, U., Passchier, C.W., Gessner, K., Güngör, T., 2003. Contrasting metamorphic evolution of metasedimentary rocks from the Çine and Selimiye nappes in the Anatolide belt, western Turkey. Journal of Metamorphic Geology 21, 699–721.

Régnier, J.L., Mezger, J.E., Passchier, C.W., 2007. Metamorphism of Precambrian–Palaeozoic schists of the Menderes core series and contact relationships with Proterozoic orthogneisses of the western Çine Massif, Anatolide belt, western Turkey. Geological Magazine 144, 67–104.

Ring, U., Gessner, K., Güngör, T., Passchier, C.W., 1999. The Menderes Massif of western Turkey and the Cycladic Massif in the Aegean – do they really correlate? Journal of Geological Society (London) 156, 3–6.

Schaltegger, U., 1994. Unravelling the pre-Mesozoic history of Aar and Gotthard massifs (Central Alps) by isotopic dating – a review. Schweizerische Mineralogische und Petrographische Mitteilungen 74, 41–51.

Schaltegger, U., Gebauer, D., 1999. Pre-Alpine geochronology of the Central, Western and Southern Alps. Schweizerische Mineralogische und Petrographische Mitteilungen 79, 79–87.

Sengör, A.M.C., Yılmaz, Y., 1981. Tethyan evolution of Turkey: a plate tectonic approach. Tectonophysics 75, 181–241.

Spry, A., 1969. Metamorphic Textures. Pergamon Press, Oxford, 350 pp.

Strömgård, K.E., 1973. Stress distribution during formation of boudinage and pressure shadows. Tectonophysics 16, 215–248.

Swanson, M.T., 1992. Late Acadian–Alleghenian transpressional deformation: evidence from asymmetric boudinage in the Casco Bay area, coastal Maine. Journal of Structural Geology 14, 323–341.